Finding the ciliary beating pattern with optimal efficiency

Natan Osterman[a,b] and Andrej Vilfan[a,c,1]

[a]J. Stefan Institute, 1000 Ljubljana, Slovenia; [b]Department of Physics, Ludwig-Maximilians University Munich, 80799 Munich, Germany; and [c]Faculty of Mathematics and Physics, University of Ljubljana, 1000 Ljubljana, Slovenia

Edited by T. C. Lubensky, University of Pennsylvania, Philadelphia, PA, and approved July 20, 2011 (received for review May 17, 2011)

We introduce a measure for energetic efficiency of biological cilia acting individually or collectively and numerically determine the optimal beating patterns according to this criterion. Maximizing the efficiency of a single cilium leads to curly, often symmetric, and somewhat counterintuitive patterns. However, when looking at a densely ciliated surface, the optimal patterns become remarkably similar to what is observed in microorganisms like Paramecium. The optimal beating pattern then consists of a fast effective stroke and a slow sweeping recovery stroke. Metachronal coordination is essential for efficient pumping and the highest efficiency is achieved with antiplectic waves. Efficiency also increases with an increasing density of cilia up to the point where crowding becomes a problem. We finally relate the pumping efficiency of cilia to the swimming efficiency of a spherical microorganism and show that the experimentally estimated efficiency of Paramecium is surprisingly close to the theoretically possible optimum.

low Reynolds number | hydrodynamics | microswimmers | metachronal waves | stroke kinematics

Many biological systems have evolved to work with a very high energetic efficiency. For example, muscle can convert the free energy of ATP hydrolysis to mechanical work with >50% efficiency (1), the F1-F0 ATP synthase converts electrochemical energy of protons to chemical energy stored in ATP molecules with even higher efficiency (2), etc. At first glance, the beating of cilia and flagella does not fall into the category of processes with such a high efficiency. Cilia are hair-like protrusions that beat in an asymmetric fashion to pump the fluid in the direction of their effective stroke (3). They propel certain protozoa, such as *Paramecium*, and also fulfill a number of functions in mammals, including mucous clearance from airways, left-right asymmetry determination, and transport of an egg cell in fallopian tubes. Lighthill (4) defines the efficiency of a swimming microorganism as the power that would be needed to drag an object of the same size with the same speed through viscous fluid, divided by the actually dissipated power. Although the efficiency defined in this way could theoretically even exceed 100% (5), the actual swimming efficiencies are of the order of 1% (6, 7). In his legendary paper on life at low Reynolds number (8) Purcell stated that swimming microorganisms have a poor efficiency, but that the energy expenditure for swimming is so small that it is of no relevance for them (he uses the analogy of "driving a Datsun [a fuel-efficient car of the period] in Saudi Arabia") (ref. 8, p. 9). Nevertheless, later studies show that swimming efficiency is important in microorganisms. In *Paramecium*, more than half of the total energy consumption is needed for ciliary propulsion (9).

When applied to ciliary propulsion, Lighthill's efficiency (4) has some drawbacks. For one, it is not a direct criterion for the hydrodynamic efficiency of cilia as it also depends on the size and shape of the whole swimmer. Besides that it is, naturally, applicable only for swimmers and not for other systems involving ciliary fluid transport with a variety of functions, like left-right asymmetry determination (10). We therefore propose a different criterion for efficiency at the level of a single cilium or a carpet of cilia. A first thought might be to define it as the volume flow rate of the transported fluid, divided by the dissipated power. However, as the flow rate scales linearly with the velocity, but the dissipation quadratically, this criterion would yield the highest efficiency for infinitesimally slow cilia, just like optimizing the fuel consumption of a road vehicle alone might lead to fitting it with an infinitesimally weak engine. Instead, like engineers trying to optimize the fuel consumption at a given speed, the well-posed question is which beating pattern of a cilium will achieve a certain flow rate with the smallest possible dissipation.

The problem of finding the optimal strokes of hypothetical microswimmers has drawn a lot of attention in recent years. Problems that have been solved include the optimal stroke pattern of Purcell's three-link swimmer (11), an ideal elastic flagellum (12), a shape-changing body (13), a two- and a three-sphere swimmer (14), and a spherical squirmer (5). Most recently, Tam and Hosoi optimized the stroke patterns of *Chlamydomonas* flagella (15). However, all these studies are still far from the complexity of a ciliary beat with an arbitrary 3D shape, let alone from an infinite field of interacting cilia. In addition, they were all performed for the swimming efficiency of the whole microorganism, whereas our goal is to optimize the pumping efficiency at the level of a single cilium, which can be applicable to a much greater variety of ciliary systems.

So we propose a cilium embedded in an infinite plane (at $z = 0$) and pumping fluid in the direction of the positive x axis. We define the volume flow rate Q as the average flux through a half-plane perpendicular to the direction of pumping (16). With P we denote the average power with which the cilium acts on the fluid, which is identical to the total dissipated power in the fluid-filled half-space. We then define the efficiency in a way that is independent of the beating frequency ω as

$$\epsilon = \frac{Q^2}{P}. \qquad [1]$$

As we show in *SI Text, section 1*, minimizing the dissipated power P for a constant volume flow rate Q is equivalent to maximizing ϵ at a constant frequency. A similar argument for swimming efficiency has already been brought forward by Avron et al. (13).

Furthermore, a general consequence of low Reynolds number hydrodynamics is that the volume flow depends only on the shape of the stroke and on the frequency, but not on the actual time dependence of the motion within a cycle. This finding is the basis of Purcell's scallop theorem (8). As a consequence, the optimum stroke always has a dissipation rate constant in time. We show this in *SI Text*, *section 2*.

We can make the efficiency ϵ completely dimensionless if we factor out the effects of the ciliary length L, the beating fre-

Author contributions: A.V. designed research; N.O. and A.V. performed research; A.V. analyzed data; and N.O. and A.V. wrote the paper.

The authors declare no conflict of interest.

This article is a PNAS Direct Submission.

[1]To whom correspondence should be addressed. E-mail: andrej.vilfan@ijs.si.

This article contains supporting information online at www.pnas.org/lookup/suppl/doi:10.1073/pnas.1107889108/-/DCSupplemental.

quency ω, and the fluid viscosity η. The velocity with which a point on the cilium moves scales with ωL and the linear force density (force per unit length) with $\eta\omega L$. The total dissipated power P, obtained by integration of the product of the velocity and linear force density over the length, then scales with $\eta\omega^2 L^3$. The volume flow rate Q scales with ωL^3. Finally, the efficiency ϵ scales with L^3/η. The dimensionless efficiency can therefore be defined as

$$\epsilon' = L^{-3}\eta\epsilon. \quad [2]$$

When optimizing the efficiency of ciliary carpets, we have to use the measures of volume flow and dissipation per unit area, rather than per cilium. We introduce the surface density of cilia ρ, which is $1/d^2$ on a square lattice. In the following we show that the volume flow generated per unit area, ρQ, is also equivalent to the flow velocity above the ciliary layer. The fluid velocity above an infinite ciliated surface namely becomes homogeneous at a distance sufficiently larger than the ciliary length and metachronal wavelength. The far field of the flow induced by a single cilium located at the origin and pumping fluid in the direction of the x axis has the form (17)

$$\mathbf{v}(x,y,z) = \mathcal{A}\frac{xz}{r^4}\hat{e}_r \quad [3]$$

with an arbitrary amplitude $\mathcal{A}$. For this field the volume flow rate is

$$Q = \int_{-\infty}^{\infty} dy \int_0^{\infty} dz v_x(x,y,z) = \frac{2}{3}\mathcal{A} \quad [4]$$

and the velocity above an infinite field of such cilia is

$$v_c = \int_{-\infty}^{\infty} dx \int_{-\infty}^{\infty} dy \rho v_x(-x,-y,z) = \frac{2\pi}{3}\rho\mathcal{A} = \pi\rho Q, \quad [5]$$

which is independent of z. In this regime, one can simplify the description of cilia by replacing them with a surface slip term with velocity v_c (18).

We now define the collective efficiency as $\epsilon_c = (\rho Q)^2/(\rho P)$ and in dimensionless form as

$$\epsilon_c' = \frac{\eta}{L}\frac{\rho^2 Q^2}{\rho P}. \quad [6]$$

ϵ_c' is a function of the beat shape, the dimensionless density ρL^2, and the metachronal coordination, which is explained later. Additionally, for a single cilium or for collective cilia the efficiency also depends on the dimensionless radius of the cilium, a/L, but this dependence is rather weak, of logarithmic order.

At this point we note that our definition of efficiency is different from that used by Gueron and Levit-Gurevich (19). They define efficiency as volume flux through a specifically chosen rectangle above the group of cilia divided by the dissipated power. Whereas this measure is useful for studying the effect of coupling and metachronal coordination (they show that the collective efficiency of a group of cilia increases with its size), it lacks the scale invariance discussed above. Gauger et al. (20) studied a model for individual and collective magnetically driven artificial cilia. Rather than introducing a single measure for the efficiency, they studied the pumping performance (which is the more relevant quantity in artificial systems) and dissipation separately. They showed that the pumping performance per cilium can be improved with the proper choice of the metachronal wave vector, whereas the dissipation per cilium remains largely constant. Both studies were limited to 2D geometry (planar cilia arranged in a linear row) and neither of them uses a scale-invariant efficiency criterion proposed here. On the other hand, Lighthill's criterion for swimming organisms shares the same scaling properties as ours (it scales with the square of the swimming velocity, divided by dissipation), but differs in definition because it measures the swimming and not the pumping efficiency. At the end we show how the two measures are related to each other for a spherical swimmer.

Our goal is to find the beating patterns that have the highest possible efficiency for a single cilium, as well as the beating patterns combined with the density and the wave vector that give the highest efficiency of a ciliated surface.

Model

We describe the cilium as a chain of N touching beads with radii a. The first bead of a cilium has the center position $\mathbf{x}_1 = (0, 0, a)$, and each next bead in the chain is located at $\mathbf{x}_{i+1} = \mathbf{x}_i + 2a(\sin\theta_i \cos\varphi_i, \sin\theta_i \sin\varphi_i, \cos\theta_i)$. The maximum curvature of the cilium is limited by the condition

$$(\mathbf{x}_{i+1} - \mathbf{x}_i)(\mathbf{x}_i - \mathbf{x}_{i-1}) \geq (2a)^2 \cos\beta_{\max}. \quad [7]$$

Naturally, beads cannot overlap with the surface ($z_i > a$) or with each other, $|\mathbf{x}_i - \mathbf{x}_j| > 2a$.

We describe the hydrodynamics using the mobility matrix formalism. If the force acting on bead i is $\mathbf{F}_i$, the resulting velocities are

$$\frac{d}{dt}\mathbf{x}_i = \sum_j M_{i,j}\mathbf{F}_j. \quad [8]$$

In this formalism, each element $M_{i,j}$ is itself a 3×3 matrix, corresponding to three spatial dimensions. In general, the above equation should also include angular velocities and torques, but they are negligible for small beads when the surface speeds due to rotational motion are much smaller than those due to translational motion. The mobility matrix is symmetric and positive definite (21). Therefore, one can always invert it to obtain the friction matrix $\Gamma = M^{-1}$, which determines the forces on particles moving with known velocities

$$\mathbf{F}_i = \sum_j \Gamma_{i,j}\dot{\mathbf{x}}_j. \quad [9]$$

If the particles were at large distances relative to their sizes, the elements of the mobility matrix would be determined by Blake's tensor (22), which represents the Green function of the Stokes flow in the presence of a no-slip boundary. In our case the condition of large interparticle distances is not fulfilled and we use the next higher approximation, which is the Rotne-Prager tensor in the presence of a boundary, as described in a previous paper (23).

The volume flow rate in the x direction, averaged over one beat period T, depends on x components of forces acting on particles and their heights z above the boundary (16):

$$Q = \frac{1}{T}\int_0^T \frac{1}{\pi\eta}\sum_i z_i(t)F_{x,i}(t)dt. \quad [10]$$

The dissipation rate is simply the total power needed to move the beads against viscous drag,

$$P = \sum_i \dot{\mathbf{x}}_i \cdot \mathbf{F}_i. \quad [11]$$

We numerically maximized the quantity Q^2/P for a set of angles $\beta_{\max}$ and different numbers of beads. We used the sequential quadratic programming algorithm (SQP) from Numerical

Algorithms Group (NAG) numerical libraries. The full details of the numerical procedure are given in *SI Text*, *section 3*.

To study the collective efficiency and metachronal coordination, we studied an array of $N_a \times N_a$ cilia (unit cell) on a square lattice with a lattice constant d. We introduced periodic boundary conditions by adding hydrodynamic interactions between particles and the representations beyond lattice boundaries. So if a certain element in the mobility matrix describing interaction between particles at $\mathbf{x}_i$ and $\mathbf{x}_j$ is $M_{i,j}(\mathbf{x}_i, \mathbf{x}_j)$, we replace it by $M'_{i,j}(\mathbf{x}_i, \mathbf{x}_j) = \sum_{p,q=-\infty}^{\infty} M_{i,j}(\mathbf{x}_i, \mathbf{x}_j + pA\hat{e}_x + qA\hat{e}_y)$. Here $A = N_a d$ denotes the size of the unit cell. For the sake of numerical efficiency, we used the full Rotne-Prager form for the first o instances ($p, q = -o, \ldots, o$) and approximated the interaction with its long-range limit, independent of the actual particle positions, for the rest (*SI Text*, *section 3*).

We expect the optimal solution to have the form of metachronal waves with a wave vector $\mathbf{k} = (k_x, k_y) = (2\pi/A)(\kappa_x, \kappa_y)$. To satisfy the periodic boundary conditions, κ_x and κ_y have to be integer numbers, e.g., between 0 and $N_a - 1$.

Results

Single-Particle Model. We first start with some simple models that are not necessarily feasible in practice, but allow important insight into how the optimum is achieved. We follow the spirit of the model used to study the synchronization of cilia (17), where we replace the cilium by a small spherical particle. There are many swimmer models building on similar assumptions, for example the three-sphere swimmer (24), and they all have in common that they assume the connections between spheres to be very thin and neglect any hydrodynamic forces acting on them.

So the first hypothetical model we study is a single sphere of radius a that can move along an arbitrary path $\mathbf{x}(\omega t)$ in the half space above the boundary, but to mimic the tip of a cilium it has to stay within the distance L of the origin, $|\mathbf{x}| \le L - a$. To simplify the calculation we also assume that the sphere is small, $a \ll L$. In this limit, we can neglect the effect of the boundary on the hydrodynamic drag, which is then always $\gamma = 6\pi\eta a$. The dissipated power is then simply $P = \gamma \dot{\mathbf{x}}^2$. Because it has to be constant in time, we can also write it as

$$P = \gamma \ell^2 / T^2 \qquad [12]$$

with ℓ denoting the total distance traveled within one cycle and T its period. The average volume flow follows from Eq. **10** as

$$Q = \frac{1}{\pi\eta T}\int_0^T z(t)\gamma\dot{x}(t)\,dt = \frac{6a}{T}\oint z dx = \frac{6Sa}{T}, \qquad [13]$$

where S is the area of the particle trajectory, projected onto the $x - z$ plane. The resulting efficiency is (Eq. **1**)

$$\epsilon = \frac{Q^2}{P} = \frac{6S^2 a}{\pi\eta\ell^2}. \qquad [14]$$

To find the optimal path, we thus have to maximize the area-to-circumference ratio of the path, while fulfilling the constraints $z > 0$ and $|\mathbf{x}| \le L$. Obviously, there is no benefit in going out of the $x - z$ plane, but there is cost associated with it. Therefore, the optimum trajectories will be planar. As in any curve that minimizes its circumference at a fixed surface area, the unconstrained segments of the trajectory have to be circle arcs. The curve has the shape shown in Fig. 1*A*. A numerical solution shows that the area-to-circumference ratio is maximal if the angle α defined in Fig. 1*A* has the value $\alpha = 0.483$. The resulting maximal efficiency in the limit $a \ll L$ is $\epsilon = 0.192\, L^2 a/\eta$, or, in dimensionless form, $\epsilon' = 0.192\, a/L$.

Solutions for finite values of a/L are shown in Fig. 1*B* and their efficiencies in Fig. 1*D*. The highest possible numerical efficiency of this model is $\epsilon' = 0.0087$, which is achieved at $a/L = 0.13$.

Another version of the single-particle model is one in which the particle has to maintain a fixed distance $(L - a)$ from the origin, while it is free to move along the surface of a sphere (Fig. 1*C*). This is an additional constraint and can therefore only reduce the achievable efficiency. As shown by the red line in Fig. 1*D*, the efficiency indeed lies somewhat below that of the model with a variable distance and reaches a maximum value of $\epsilon' = 0.0065$.

***N* Particles, Stiff Cilium.** The next minimalistic model we study is a stiff cilium: a straight chain of N beads with radius a and a total length of $L = 2Na$ that can rotate freely around the center of the first bead. The problem is related to artificial cilia driven by a magnetic field (20, 23, 25) in which the orientation of the cilium largely (although not completely) follows the direction of

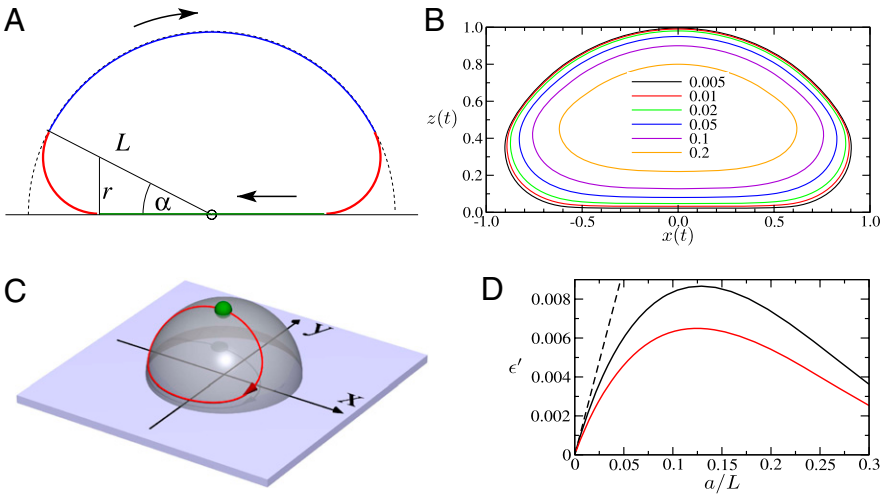

Fig. 1. Optimal trajectories of the one-particle model. (*A*) Idealized case of a small particle restricted to $|\mathbf{x}| < L$. The solution consists of piecewise circular arcs, determined by geometric parameters α and r/L. (*B*) Numerical solutions for finite-sized particles, plotted for different ratios a/L. (*C*) Optimal path for a particle at a constant distance from the origin, $|\mathbf{x}| = L - a$, with $a = 0.1L$. The transparent hemisphere symbolizes the surface on which the particle can move. (*D*) Dimensionless efficiency ϵ' as a function of the dimensionless particle radius a/L. The black line shows the model with variable distance and the red line that with a fixed distance from the origin. The dashed line shows the limit of small radii ($a \ll L$), $\epsilon' = 0.192a/L$.

the magnetic field. A related optimization has been performed by Smith et al. (16), but with two important differences. First, Smith et al. optimize the volume flow alone and not the efficiency. Their optimal stroke therefore touches the surface during the recovery stroke, whereas ours has to keep some distance to limit the dissipation. Second, they restrict themselves to cilia beating along tilted cones, whereas we allow any arbitrary pattern.

The motion of a stiff cilium on its optimal trajectory is shown in Fig. 2*A*. The path of its tip closely resembles that of a single sphere at a fixed radius. The resulting dimensionless efficiency for $N = 20$ beads is $\epsilon' = 0.00535$.

***N* Particles, Flexible Cilium.** As the next level of complexity, and at the same time the first realistic description of biological cilia, we now study a flexible cilium consisting of N spherical particles (we use $N = 10$ and $N = 20$). The bending angle per particle is restricted to $\beta_{\max}$ (Eq. **7**). Such a constraint is necessary for two reasons. For one, the curvature of a biological cilium is restricted by the bending rigidity of the axoneme. In addition, our N-particle model veritably represents a continuous cilium only if the curvature radius is sufficiently larger than the size of a sphere. Examples of beating patterns obtained by numerical optimization are shown in Fig. 2 *B* and *C*. Fig. 2*D* shows the dimensionless efficiency ϵ' as a function of $\beta_{\max}$.

It is instructive to look at fundamental symmetries of the problem at this point. First, as in any of the problems studied here, it is symmetric upon reflection $y \to -y$. For every clockwise beat, there is an equivalent counterclockwise beat with the same efficiency. All cycles discussed here spontaneously break the y symmetry. In addition, the equations are invariant upon reflection $x \to -x$ with simultaneous time reversal, $t \to -t$. This symmetry can be broken or not at the efficiency maximum. Interestingly, whether it is broken depends on the allowed bending between adjacent elements $\beta_{\max}$. For example, the solution shown in Fig. 2*B* is xt symmetric, whereas the one in Fig. 2*C* is not.

Multiple Cilia and Metachronal Waves. We solve the optimization problem of $N_a \times N_a$ cilia ($N_a = 12$) with periodic boundary conditions by imposing a wave vector (k_x, k_y), finding the optimal solution for that vector, and repeating the procedure for $N_a \times N_a$ wave vectors. Examples of optimal solutions for six different wave vectors are shown in Fig. 3 *A–F*. The efficiency ϵ'_c as a function of the wave vector is shown in Fig. 3*G*. Note that all solutions determined in this section are for counterclockwise beating (viewed from above). For clockwise strokes the y component of the wave vector would have the opposite sign. Optimal solutions for four different values of the intercilliary distance d are shown in Fig. 4 *A–D* and the optimal efficiency as a function of d in Fig. 4*E*.

Fig. 3*G* shows that the efficiency depends more strongly on the longitudinal (k_x) component of the wave vector than on the lateral one (k_y). This finding could partly be due to the nature of the hydrodynamic interaction, which is stronger in the longitudinal direction, and partly because the cilia exert larger motion in the longitudinal direction and therefore come closer to their neighbors along the x axis. Antiplectic metachronal waves (waves propagate in the opposite direction from the fluid pumping) generally have a higher efficiency than symplectic, but the fine structure is much more complex. For low ciliary densities, the optimal solution is found for waves propagating along the x axis. For higher densities solutions with a positive k_x are more efficient, which means that the waves are dexio-antiplectic. Efficiency also grows with increasing density. However, when the intercilliary distance reaches $d = 0.25L$, crowding becomes a problem and the efficiency drops again. At even higher densities the solution becomes increasingly difficult to find because of the complicated topology of densely packed cilia. Another problem is that the wavelength of the optimal solution, relative to the lattice constant, becomes increasingly long at high densities, which would require a unit cell larger than 12×12 used in our calculations.

Swimming Efficiency of a Ciliated Microorganism. We can finally use these results to estimate the maximum possible swimming efficiency of a ciliated microorganism. For the sake of simplicity, we assume that the swimmer has a spherical shape with radius R. According to Lighthill's definition, the swimming efficiency is defined as

$$\epsilon_L = \frac{6\pi\eta R V^2}{P_{tot}}, \qquad [15]$$

where V is the velocity and P_{tot} the total dissipated power (4). Assuming that the layer of cilia is thin in comparison with the size of the organism ($L \ll R$), the swimming velocity V can be calculated as (18, 26)

$$V = \frac{1}{4\pi R^2}\int \mathbf{v} d^2 s = \frac{1}{4\pi}\int_0^\pi v(\theta) 2\pi \sin^2\theta d\theta. \qquad [16]$$

Here $v(\theta)$ is the propulsion velocity above the ciliated layer. The dissipation can be expressed as

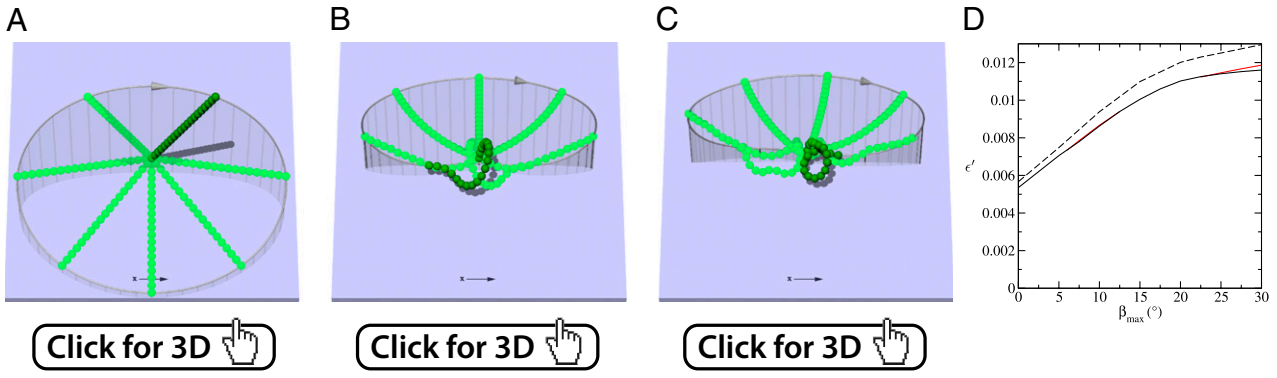

Fig. 2. Optimal beating patterns of a cilium consisting of $N = 20$ particles with different allowed bending angles $\beta_{\max}$. The gray surface shows the projection of the tip trajectory on the $x - y$ plane. (*A*) A stiff cilium, $\beta_{\max} = 0$. (*B*) A flexible cilium, $\beta_{\max} = 20°$. The optimal stroke is symmetric in the x direction. (*C*) Flexible cilium, $\beta_{\max} = 30°$. The symmetry in the x direction is broken. (*D*) Dimensionless efficiency ϵ' as a function of $\beta_{\max}$. The black line shows the optimal symmetric solution and the red line the asymmetric solution in cases where it is more efficient. The dashed line shows the maximum efficiency for $N = 10$ and double $\beta_{\max}$ (corresponding to the same curvature).

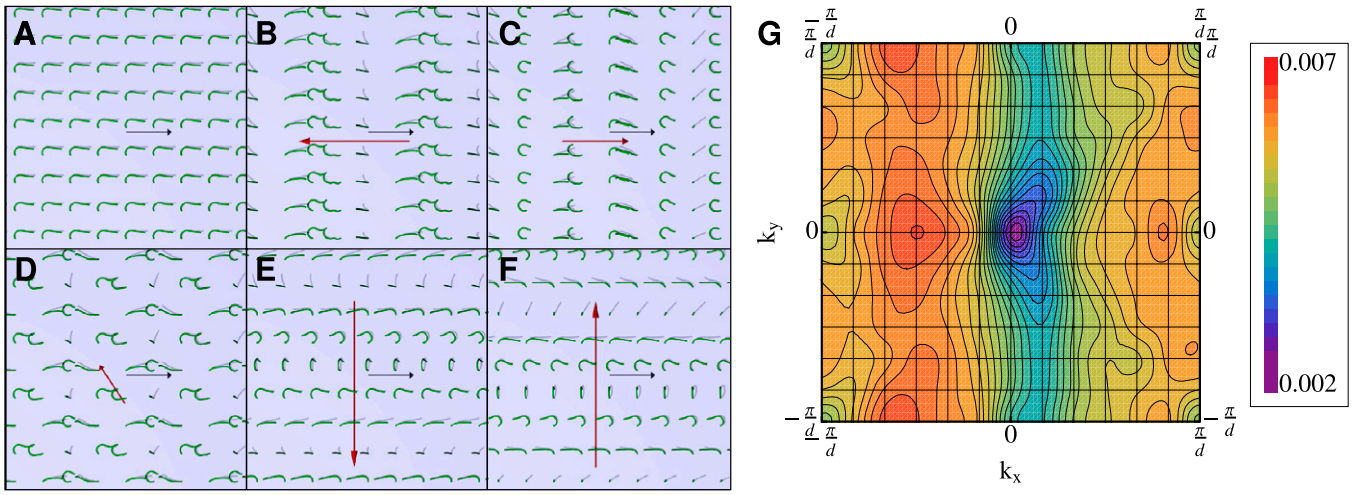

Fig. 3. Optimal solutions at fixed wave vectors for interciliary distance $d = 1.0 \times L$, $N = 20$, $\beta_{max} = 15°$, and $N_a = 12$. (*A*–*F*) Optimal solutions for wave vectors $(k_x, k_y) = (0, 0)$ (*A*), $(-\pi/(2d), 0)$ (*B*), $(5\pi/(6d), 0)$ (*C*), $(-2\pi/(3d), \pi/d)$ (*D*), $(0, -\pi/(3d))$ (*E*), and $(0, \pi/3d)$) (*F*). The blue arrow (*x* axis) denotes the direction of pumping and the red arrow the wavelength and direction of metachronal wave propagation. (*G*) Efficiency ϵ_c' (red color represents high efficiency) as a function of the wave vector (k_x, k_y). The maximum efficiency is in this case achieved for $\mathbf{k} = (-\pi/(2d), 0)$ and antiplectic waves are generally more efficient than symplectic ones. The synchronous solution (0, 0) represents the global minimum of efficiency.

$$P_{\text{tot}} = \int \rho P d^2 s = \int_0^\pi \rho P(\theta) 2\pi R^2 \sin\theta d\theta = \frac{2R^2\eta}{\pi\epsilon_c' L}\int_0^\pi v^2(\theta)\sin\theta d\theta. \quad [17]$$

In the second equality we used the definition (Eq. **6**), as well as the relationship between v and ρQ (Eq. **5**). To obtain the maximum V at a given P_{tot}, the two functional derivatives should be related through a Lagrange multiplier

$$\frac{\delta V[v]}{\delta v(\theta)} = \lambda \frac{\delta P_{\text{tot}}[v]}{\delta v(\theta)}, \quad [18]$$

which is fulfilled if the angular dependence has the form $v(\theta) = v_0 \sin\theta$. This result leads to

$$V = \frac{2}{3} v_0 \quad [19]$$

and

$$P_{\text{tot}} = \frac{8\eta R^2 v_0^2}{3\pi\epsilon_c' L}. \quad [20]$$

Together, these equations give Lighthill's efficiency

$$\epsilon_L = \pi^2 \frac{L}{R}\epsilon_c'. \quad [21]$$

With a maximum $\epsilon_c' \approx 0.016$ and a typical ratio $L/R \approx 0.1$, we obtain $\epsilon_L \approx 0.016$.

For comparison, an optimized envelope model yields an efficiency ~3% with the same parameters (if we translate the ciliary length into maximal displacement of the envelope) (5), which shows that the latter is a relatively good approximation for cilia if they operate close to the optimal way.

Discussion

We introduced a scale invariant efficiency measure for the fluid pumping by cilia and started with optimizing three simple in-

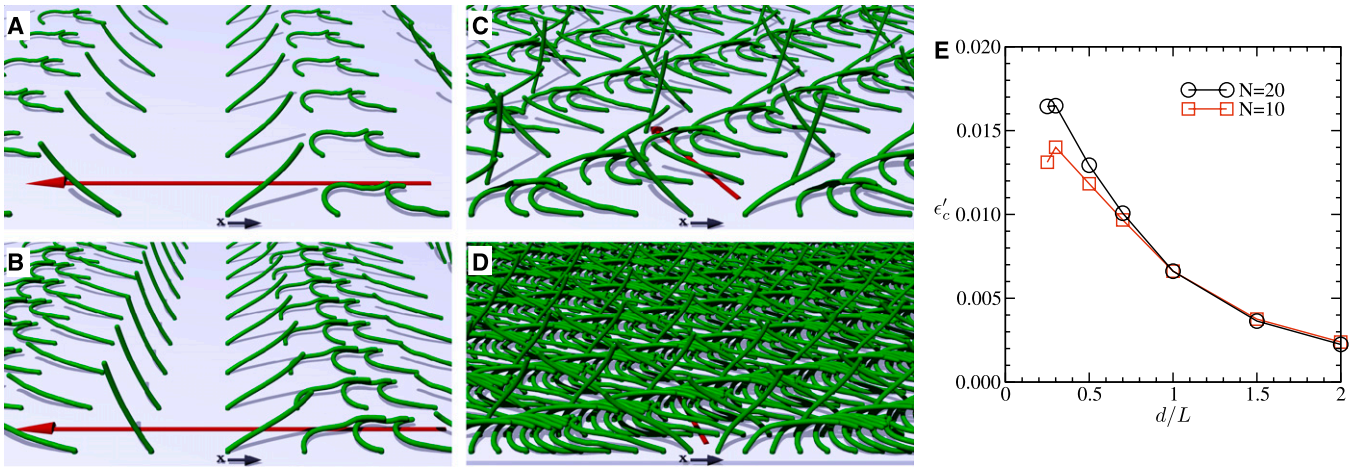

Fig. 4. Optimal solutions for various interciliary distances: $d = 1.0L$ (*A*), $d = 0.7L$ (*B*), $d = 0.5L$ (*C*), and $d = 0.25L$ (*D*). For reasons of clarity the front rows of cilia are omitted and instead of individual spheres used in the calculation a tube connecting them is shown. (*E*) Highest efficiency ϵ_c' as a function of the interciliary distance d for cilia consisting of $N = 20$ (circles) and $N = 10$ (squares) spheres. For $N = 10$, we set $\beta_{max} = 30°$ to allow the same maximum curvature.

structive systems: a free sphere, a sphere at a constant distance from the origin, and a stiff cilium. Of those three, the free sphere can reach the highest efficiency. However, they are all topped by a flexible cilium. The thickness of a cilium has only a small effect on its efficiency, which strengthens our choice to describe the cilium as a chain of beads. Depending on the allowed bending, the flexible cilium can have different shapes of the optimal beating pattern. In most cases the cilium curls up during the recovery stroke, rather than sweeping along the surface. Such shapes appear "unnatural" if we compare them with those observed in microorganisms (27).

However, the collective optimization of ciliary carpets leads to beating patterns that are strikingly similar to what is observed in many ciliated microorganisms. Unlike isolated cilia, they contain a recovery stroke during which they sweep along the surface. This result is primarily due to the fact that beating patterns that are optimal for a single cilium (e.g., as shown in Fig. 2*B*) are not possible on a dense grid due to steric hindrance. The sweeping recovery stroke, on the other hand, allows dense stacking of cilia (best seen in Fig. 4*D*), which further reduces drag as well as backward flow. The optimal effective stroke becomes significantly faster than the recovery stroke. Whereas a single cilium reaches its highest efficiency if the effective stroke takes ∼45% of the cycle, the optimal fraction is ∼20–25% for densely packed cilia. A similar ratio has been observed in *Paramecium* (28). The distance between adjacent cilia in *Paramecium* is between $0.15L$ and $0.25L$ (29), consistent with the predicted optimum around $d = 0.25L$. It is interesting that the efficiency of any other wave vector is higher than the efficiency of the synchronous solution (wave vector 0). This result is in agreement with some previous simpler, one-dimensional models (20), but has not yet been shown on a 2D lattice. We also find that antiplectic waves are generally more efficient than symplectic, although symplectic solutions with a relatively high efficiency exist, too. For high densities and cilia beating counterclockwise, the waves become almost dexioplectic (meaning that the effective stroke points to the right of the wave propagation) and the wavelength becomes similar to the cilium length L—both findings are in agreement with observations on *Paramecium* (30, 3). For cilia beating clockwise, laeoplectic waves would be more efficient, which is indeed observed (31). Although the effect of thickness is small, it is interesting to note that thicker cilia have a slightly higher efficiency when isolated or at low surface densities, but are outperformed by thinner cilia at high densities.

The total energetic efficiency of swimming in *Paramecium* has been measured as 0.078% (9). This number includes losses in metabolism and force generation—the hydrodynamic swimming efficiency alone has been estimated as 0.77%. This number comes close (by a factor of 2) to our result for the maximally possible Lighthill efficiency of a spherical ciliated swimmer, $\epsilon_L \approx 0.016$. A biflagellate swimmer like *Chlamydomonas* has a lower theoretical efficiency of 0.008 (15), but it is still within the same order of magnitude.

Although efficiencies <1% seem low, we have shown that *Paramecium* still works remarkably close to the maximum efficiency that can be achieved with its length of cilia. Whereas longer cilia might have a higher swimming efficiency, there are other considerations that are not included in this purely hydrodynamic study. For example, the bending moments and the power output per ciliary length can be limiting (32). Thus, our study shows that at least for ciliates like *Paramecium*, Purcell's view that efficiency is irrelevant for ciliary propulsion has to be revisited. Efficiency of swimming does matter for them, and in their own world they have well evolved to swim remarkably close to the optimal way.

ACKNOWLEDGMENTS. We have benefited from fruitful discussions with Frank Jülicher. This work was supported by the Slovenian Office of Science (Grants P1-0099, P1-0192, J1-2209, J1-2200, and J1-0908).

1. Kushmerick MJ, Davies RE (1969) The chemical energetics of muscle contraction. II. The chemistry, efficiency and power of maximally working sartorius muscles. Appendix. Free energy and enthalpy of atp hydrolysis in the sarcoplasm. *Proc R Soc Lond B Biol Sci* 174:315–353.
2. Yoshida M, Muneyuki E, Hisabori T (2001) ATP synthase—a marvellous rotary engine of the cell. *Nat Rev Mol Cell Biol* 2:669–677.
3. Sleigh MA, ed (1974) *Cilia and Flagella* (Academic, London).
4. Lighthill MJ (1952) On the squirming motion of nearly spherical deformable bodies through liquids at very small Reynolds numbers. *Commun Pure Appl Math* 5:109–118.
5. Michelin S, Lauga E (2010) Efficiency optimization and symmetry-breaking in a model of ciliary locomotion. *Phys Fluids* 22:111901.
6. Purcell EM (1997) The efficiency of propulsion by a rotating flagellum. *Proc Natl Acad Sci USA* 94:11307–11311.
7. Chattopadhyay S, Moldovan R, Yeung C, Wu XL (2006) Swimming efficiency of bacterium Escherichia coli. *Proc Natl Acad Sci USA* 103:13712–13717.
8. Purcell EM (1977) Life at low Reynolds number. *Am J Phys* 45:3–11.
9. Katsu-Kimura Y, Nakaya F, Baba SA, Mogami Y (2009) Substantial energy expenditure for locomotion in ciliates verified by means of simultaneous measurement of oxygen consumption rate and swimming speed. *J Exp Biol* 212:1819–1824.
10. Supatto W, Fraser SE, Vermot J (2008) An all-optical approach for probing microscopic flows in living embryos. *Biophys J* 95:L29–L31.
11. Tam D, Hosoi AE (2007) Optimal stroke patterns for Purcell's three-link swimmer. *Phys Rev Lett* 98:068105.
12. Spagnolie SE, Lauga E (2010) The optimal elastic flagellum. *Phys Fluids* 22:031901.
13. Avron JE, Gat O, Kenneth O (2004) Optimal swimming at low Reynolds numbers. *Phys Rev Lett* 93:186001.
14. Alouges F, DeSimone A, Lefebvre A (2009) Optimal strokes for axisymmetric microswimmers. *Eur Phys J E Soft Matter* 28:279–284.
15. Tam D, Hosoi AE (2011) Optimal feeding and swimming gaits of biflagellated organisms. *Proc Natl Acad Sci USA* 108:1001–1006.
16. Smith DJ, Blake JR, Gaffney EA (2008) Fluid mechanics of nodal flow due to embryonic primary cilia. *J R Soc Interface* 5:567–573.
17. Vilfan A, Jülicher F (2006) Hydrodynamic flow patterns and synchronization of beating cilia. *Phys Rev Lett* 96:058102.
18. Jülicher F, Prost J (2009) Generic theory of colloidal transport. *Eur Phys J E Soft Matter* 29:27–36.
19. Gueron S, Levit-Gurevich K (1999) Energetic considerations of ciliary beating and the advantage of metachronal coordination. *Proc Natl Acad Sci USA* 96:12240–12245.
20. Gauger EM, Downton MT, Stark H (2009) Fluid transport at low Reynolds number with magnetically actuated artificial cilia. *Eur Phys J E Soft Matter* 28:231–242.
21. Happel J, Brenner H (1983) *Low Reynolds Number Hydrodynamics* (Kluwer, Dordrecht, The Netherlands).
22. Blake JR (1971) A note on the image system for a stokeslet in a no-slip boundary. *Proc Camb Philos Soc* 70:303–310.
23. Vilfan M, et al. (2010) Self-assembled artificial cilia. *Proc Natl Acad Sci USA* 107: 1844–1847.
24. Najafi A, Golestanian R (2004) Simple swimmer at low Reynolds number: Three linked spheres. *Phys Rev E Stat Nonlin Soft Matter Phys* 69:062901.
25. Downton MT, Stark H (2009) Beating kinematics of magnetically actuated cilia. *Europhys Lett* 85:44002.
26. Stone HA, Samuel AD (1996) Propulsion of microorganisms by surface distortions. *Phys Rev Lett* 77:4102–4104.
27. Brennen C, Winet H (1977) Fluid mechanics of propusion by cilia and flagella. *Annu Rev Fluid Mech* 9:339–398.
28. Gueron S, Levit-Gurevich K, Liron N, Blum JJ (1997) Cilia internal mechanism and metachronal coordination as the result of hydrodynamical coupling. *Proc Natl Acad Sci USA* 94:6001–6006.
29. Sleigh MA (1969) Coordination of the rhythm of beat in some ciliary systems. *Int Rev Cytol* 25:31–54.
30. Machemer H (1972) Ciliary activity and the origin of metachrony in Paramecium: Effects of increased viscosity. *J Exp Biol* 57:239–259.
31. Gheber L, Priel Z (1990) On metachronism in ciliary systems: A model describing the dependence of the metachronal wave properties on the intrinsic ciliary parameters. *Cell Motil Cytoskeleton* 16:167–181.
32. Sleigh MA, Blake JR (1977) Methods of ciliary propulsion and their size limitations. *Scale Effects in Animal Locomotion*, ed Pedley TJ (Academic, London), pp 243–256.